Interaction of Cholesterol with a Docosahexaenoic Acid-Containing Phosphatidylethanolamine: Trigger for Microdomain/Raft Formation?†

Saame Raza Shaikh,‡,§ Vadim Cherezov,|| Martin Caffrey,|| William Stillwell,‡,§ and Stephen R. Wassall*,§,⊥

Department of Biology, Indiana University Purdue University Indianapolis, 723 West Michigan Street, Indianapolis, Indiana 46202-5132, Biochemistry, Biophysics, and Chemistry, The Ohio State University, Columbus, Ohio 43210-1173, Department of Physics, Indiana University Purdue University Indianapolis, 402 North Blackford Street, Indianapolis, Indiana 46202-3273, and Medical Biophysics Program, Indiana University School of Medicine, 635 Barnhill Drive, Indianapolis, Indiana 46202-5122

Received May 30, 2003; Revised Manuscript Received July 30, 2003

ABSTRACT: Docosahexaenoic acid (DHA, 22:6) containing phospholipids have been postulated to be involved in promoting lateral segregation within membranes into cholesterol- (CHOL-) rich and CHOL-poor lipid microdomains. Here we investigated the specific molecular interactions of phospholipid bilayers composed of 1-[$^2H_{31}$]palmitoyl-2-docosahexaenoyl-*sn*-glycero-3-phosphoethanolamine (16:0-22:6PE-d_{31}) or 1-[$^2H_{31}$]palmitoyl-2-oleoyl-*sn*-glycero-3-phosphoethanolamine (16:0-18:1PE-d_{31}) with equimolar CHOL using solid-state ^{2}H NMR spectroscopy and low- and wide-angle X-ray diffraction (XRD). Moment analysis of ^{2}H NMR spectra obtained as a function of temperature reveals that the main chain melting transition and the lamellar-to-inverted hexagonal (H_{II}) phase transition of 16:0-22:6PE-d_{31} remain in the presence of equimolar CHOL, whereas addition of equimolar CHOL essentially obliterates the gel-to-liquid crystalline transition of 16:0-18:1PE-d_{31}. ^{2}H NMR order parameter measurements show that the addition of equimolar CHOL in the lamellar liquid crystalline phase causes a smaller increase in order for the perdeuterated *sn*-1 chain by 22% for 16:0-22:6PE-d_{31} as opposed to 33% for 16:0-18:1PE-d_{31}. XRD experiments determined markedly lower solubility of 32 ± 3 mol % for CHOL in 16:0-22:6PE bilayers in contrast to the value of ∼51 mol % for 16:0-18:1PE. Our findings provide further evidence that cholesterol has a low affinity for DHA-containing phospholipids and that this reduced affinity may serve as a mechanism for triggering the formation of lipid microdomains such as rafts.

In mammalian cells, approximately 90% of the total cellular cholesterol is found within the plasma membrane (*1*) where it can comprise in excess of 50 mol % of the lipid species (*2*). This high abundance has prompted extensive studies into its role in membrane structure and function (*3*). It is well accepted that cholesterol orders liquid crystalline state lipids by diminishing acyl chain trans−gauche isomerizations, and recent evidence indicates preferential association with saturated acyl chains of phospholipids (*4*, *5*). Much of the understanding of cholesterol's effect on membrane phase behavior has come from model membrane studies of varying mixtures of homoacid saturated or heteroacid saturated−monounsaturated phosphatidylcholine (PC)[1] membranes and cholesterol. Far less is understood about interactions of the sterol with polyunsaturated acyl chains, especially those associated with phosphatidylethanolamine (PE) headgroups. We (*4*, *6*−*8*) and others (*5*, *9*) have previously suggested that acyl chain polyunsaturation may trigger the formation of membrane microdomains including lipid rafts. Specifically, a reduced affinity between the polyunsaturated acyl chain and cholesterol has been hypothesized to serve as a lipid-driven mechanism for lateral segregation into cholesterol-rich and cholesterol-poor microdomains (*10*). Here we further explore this hypothesis by investigating cholesterol's interactions with a heteroacid saturated−polyunsaturated PE vs a saturated−monounsaturated PE using solid-state ^{2}H NMR spectroscopy and low- and wide-angle X-ray diffraction (XRD).

The motivation for investigating cholesterol−PE interactions at a molecular level comes from the lipid raft hypothesis. Lipid rafts are sphingolipid−cholesterol-rich microdomains postulated to serve as platforms for cellular signaling proteins (*11*, *12*). They are generally presumed to be in a

† This work was supported by grants from the National Institutes of Health (RO1CA57212 and GM61070) and the National Science Foundation (DIR 9016683 and DBI 9981990).

* Corresponding author. E-mail: swassall@iupui.edu. Tel: (317) 274-6908. Fax: (317) 274-2393.

‡ Department of Biology, Indiana University Purdue University Indianapolis.

§ Indiana University School of Medicine.

|| The Ohio State University.

⊥ Department of Physics, Indiana University Purdue University Indianapolis.

[1] Abbreviations: CHOL, cholesterol; DSC, differential scanning calorimetry, H_{II}, inverted hexagonal phase; L_α, lamellar liquid crystalline phase; L_β, lamellar gel phase; l_d, liquid disordered phase; l_o, liquid ordered phase; PC, phosphatidylcholine; 16:0-22:6PE, 1-palmitoyl-2-docosahexaenoyl-*sn*-glycero-3-phosphoethanolamine; PE, phosphatidylethanolamine; 16:0-18:1PE, 1-palmitoyl-2-oleoyl-*sn*-glycero-3-phosphoethanolamine; SM, sphingomyelin; T_h, lamellar-to-hexagonal phase transition temperature; T_m, gel-to-liquid crystalline phase transition temperature.

10.1021/bi034931+ CCC: $25.00
Published on Web 09/25/2003

liquid ordered (l_o) phase, an intermediate state between the lamellar liquid crystalline (L_α) and gel (L_β) states, also respectively known as liquid disordered (l_d) and solid ordered (s_o) states (*13*). The saturated acyl chains found in the l_o state show order similar to the L_β phase but are characterized by fast axial rotation and high lateral mobility more akin to the L_α state (*14*). Molecular evidence for lipid raft formation has come in part from model membrane studies employing mixtures of cholesterol, sphingolipids, and PCs. However, relatively little work has been done to characterize raft formation involving PEs which constitute the second most abundant type of phospholipid in the mammalian plasma membrane. Proteins anchored to the cytoplasmic leaflet of the plasma membrane, where PEs are found abundantly, have been identified in the lipid raft fraction when isolated using the biochemical detergent extraction method (*15*). Thus, it is of interest to investigate the role of cholesterol in modulating membrane phase behavior with PE lipid species in order to better understand raft formation.

PEs usually exist as *sn*-1 saturated, *sn*-2 monounsaturated species in the plasma membrane. Early differential scanning calorimetry (DSC) studies suggested that cholesterol has a reduced affinity for PEs relative to PCs and sphingolipids (*16*). This finding was confirmed by a recently developed cyclodextrin assay of partition coefficients for cholesterol in unilamellar vesicles (*17*). However, ^{2}H NMR work has shown that l_o phases can be formed between cholesterol and PEs (*18*). Spectra were reported demonstrating, for example, that 1-[$^2H_{31}$]palmitoyl-2-oleoyl-*sn*-glycero-3-phosphoethanolamine (16:0-18:1PE-d_{31}) bilayers containing a mole fraction of cholesterol (χ_{CHOL}) >0.35 forms an l_o phase similar to that of PCs. Less is known about the interactions between cholesterol and a *sn*-1 saturated, *sn*-2 polyunsaturated PE. In the present study, we utilize a PE with palmitic acid at the *sn*-1 position and docosahexaenoic acid (DHA) at the *sn*-2 position. DHA at the *sn*-2 position in a PE was selected since our previous work demonstrated that DHA incorporates preferentially into PEs in T27A tumor cells (*19*). With 22 carbons and 6 double bonds, DHA represents the extreme example of a polyunsaturated fatty acid commonly found in the plasma membrane (*8*).

The focus for this study is the suggestion that DHA-containing phospholipids partition into cholesterol-poor domains and may induce lateral phase separations between cholesterol-rich and cholesterol-poor microdomains (*8*, *9*). Support was provided by our earlier investigation of PE/sphingomyelin (SM)/cholesterol (1/1/1) mixtures that presented preliminary data implying sterol-induced segregation with 1-palmitoyl-2-docosahexaenoyl-*sn*-glycero-3-phosphoethanolamine (16:0-22:6PE) but not with 1-palmitoyl-2-oleoyl-*sn*-glycero-3-phosphoethanolamine (16:0-18:1PE) (*7*). Here we establish a marked difference in the effect of cholesterol on a DHA-containing PE in comparison to an oleic acid-containing PE. Our experiments employ solid-state ^{2}H NMR spectroscopy to characterize the phase behavior of 1-[$^2H_{31}$]palmitoyl-2-docosahexaenoyl-*sn*-glycero-3-phosphoethanolamine (16:0-22:6PE-d_{31}) versus 16:0-18:1PE-d_{31} in the absence or presence of equimolar cholesterol over a wide temperature range. Corroborating low- and wide-angle X-ray diffraction (XRD) determines the sterol's solubility in 16:0-22:6PE and 16:0-18:1PE bilayers in the lamellar liquid crystalline phase. The findings in this study are discussed in relation to existing models of DHA-containing phospholipid−cholesterol phase separations.

EXPERIMENTAL PROCEDURES

Materials. 16:0-18:1PE, 16:0-18:1PE-d_{31}, 16:0-22:6PE, and 16:0-22:6PE-d_{31} were purchased from Avanti Polar Lipids (Alabaster, AL). Cholesterol (CHOL) was obtained from Sigma Chemical Co. (St. Louis, MO). Lipid purity was assured with thin-layer chromatography. Lipid and cholesterol concentrations were quantified using phosphate and gravimetric analyses, respectively. Deuterium-depleted H_2O (DDW) used in the ^{2}H NMR experiments was purchased from Isotec Inc. (Miamisburg, OH).

^{2}H NMR Sample Preparation. ^{2}H NMR samples were prepared as previously described (*7*). All manipulation of samples containing DHA was performed in a glovebox under a nitrogen atmosphere to control for oxidation. Briefly, lipid mixtures were codissolved in chloroform, and the solvent was evaporated under a gentle stream of nitrogen gas. The samples were placed under vacuum for 12 h to ensure the removal of trace organic solvent. The lipid mixtures were then hydrated to 50 wt % with 50 mM Tris buffer (pH 7.5) and vigorously vortexed for ~5 min. Excess H_2O (~2 mL) was added to the samples to enable pH adjustment. After pH correction, the samples were frozen in dry ice and lyophilized once at ~50 mTorr. The lyophilization process was repeated two more times in the presence of excess (2 mL) DDW to remove naturally abundant ^{2}HHO. After finally hydrating the powders to 50 wt %, the resultant aqueous dispersions were transferred to 5 mm glass NMR tubes which were sealed with a Teflon-coated plug. Samples were stored at −20 °C when not in use and were allowed to equilibrate to room temperature for ~1 h prior to experimentation. Lipid−cholesterol samples prepared in this manner are considered to be homogeneously mixed prior to hydration. We have compared phospholipid/cholesterol samples prepared as described here (*10*) and by the low-temperature trapping (LTT) method (*20*) designed to ensure that lipids do not demix during removal of the solvent. Both methods yielded nearly identical results that agree within experimental uncertainty.

^{2}H NMR Spectroscopy. Solid-state ^{2}H NMR spectroscopy was conducted as described before (*7*, *10*, *21*). Spectra were acquired on a home-built spectrometer operating at a resonant frequency of 27.6 MHz. A double resonance probe (Cryomagnet Systems, Inc., Indianapolis, IN) with a 5 mm transverse mounted coil and temperature control was utilized. Temperature was regulated (±0.5 °C) with a Love Controls (1600 series) temperature controller (Michigan City, IN).

Analysis of ^{2}H NMR Spectra. Moments M_n were calculated from ^{2}H NMR spectra for the perdeuterated *sn*-1 acyl chain of 16:0-22:6PE-d_{31} or 16:0-18:1PE-d_{31} with

$$M_n = \frac{\int_{-\infty}^{\infty} |\omega^n| f(\omega)\, d\omega}{\int_{-\infty}^{\infty} f(\omega)\, d\omega} \qquad (1)$$

where ω is the frequency with respect to the central Larmor frequency ω_0, $f(\omega)$ is the line shape, and n is the order of the spectral moment (*22*). In practice, the integral is a summation over the digitized data. The expression

$$M_1 = \frac{\pi}{\sqrt{3}}\left(\frac{e^2qQ}{h}\right)|\bar{S}_{CD}| \quad (2)$$

relates the first moment M_1 to the average order parameter $\bar{S}_{CD}$ of the perdeuterated palmitic chain at the *sn*-1 position in the lamellar phase via the static quadrupolar coupling constant $(e^2qQ/h) = 167$ kHz. A factor of $^1/_2$ was introduced into the right-hand side of eq 2 relating M_1 to $\bar{S}_{CD}$ for lipids in the inverted hexagonal H_{II} phase to account for additional line narrowing due to rapid diffusion around the cylindrical structures that comprise the H_{II} phase (*23*).

Spectra for 16:0-22:6PE-d_{31} and 16:0-18:1PE-d_{31} were also FFT depaked to enhance resolution. The depaking procedure numerically deconvolutes the powder pattern signal to a spectrum representative of a planar membrane of single alignment (*24*). The depaked spectra consist of doublets with quadrupolar splittings $\Delta\nu(\vartheta)$ that in the lamellar liquid crystalline phase relate to order parameters by

$$\Delta\nu(\theta) = \frac{3}{2}\left(\frac{e^2qQ}{h}\right)|S_{CD}|P_2(\cos\theta) \quad (3)$$

where $\vartheta = 0°$ is the angle the normal to the membrane surface makes with the magnetic field and $P_2(\cos\theta)$ is the second-order Legendre polynomial. Smoothed profiles of order along the perdeuterated palmitoyl *sn*-1 chain were then constructed assuming monotonic variation toward the disordered center of the bilayer (*25*).

XRD Sample Preparation. XRD samples were prepared from 15 to 20 mg of varying mole ratios of 16:0-22:6PE/CHOL or 16:0-18:1PE/CHOL as described previously (*10*). The procedure corresponds to that employed for ^{2}H NMR samples, except only a single lyophilization was required and the final mixing was achieved by forcing the sample back and forth between the narrow constrictions of two Hamilton syringes. The resultant aqueous dispersions in 50 wt % Tris buffer (pH 7.5) were transferred to 1 mm outside diameter X-ray capillary tubes (Charles Supper Co., Natick, MA) that were flame-sealed followed by a bead of quick-drying epoxy to ensure hermetic sealing. All samples were stored in dry ice and equilibrated at 20 °C for 1 h prior to X-ray diffraction measurements.

XRD Measurements. XRD experiments were performed as previously described (*10*). Cholesterol, in excess of the solubility limit, phase separates from membranes and forms monohydrate crystals which may be quantified by detecting the associated, characteristic second-order diffraction peaks (*10*, *20*). Their respective reciprocal and real spacings are (002) 0.3701 Å^{-1}, 17.0 Å; (020) 1.033 Å^{-1}, 6.079 Å; and (200) 1.044 Å^{-1}, 6.015 Å (*26*). The combined integrated intensities of these reflections (normalized with respect to the integrated intensity of the lipid wide-angle peak) were plotted against the total concentration of cholesterol added. Linear extrapolation to zero intensity was used to determine cholesterol solubility, usually with better than ±3 mol % accuracy.

RESULTS

Phase Behavior of 16:0-22:6PE-d_{31} vs 16:0-18:1PE-d_{31} in the Absence and Presence of Equimolar Cholesterol. The different phase states adopted by 50 wt % aqueous dispersions of 16:0-22:6PE-d_{31} and 16:0-18:1PE-d_{31} in 50 mM Tris (pH 7.5) were identified using ^{2}H NMR spectroscopy. ^{2}H NMR spectra illustrating that 16:0-22:6PE-d_{31} is in the L_β, L_α, and H_{II} phases at −5, 7.5, and 40 °C, respectively are shown in Figure 1a−c. The spectrum at −5 °C (Figure 1a) is a featureless broad spectrum typical of the L_β lamellar gel phase where the saturated chains are all trans and reorient slowly (*22*, *27*). A spectrum indicative of fast axial reorientation of acyl chains in the L_α lamellar liquid crystalline state is observed at 7.5 °C (Figure 1b). The well-defined edges at ±17 kHz correspond to the plateau region of almost constant order in the upper part of the *sn*-1 perdeuterated acyl chain. The less ordered methylenes in the lower part of the acyl chain give rise to individual peaks in the spectrum, and the highly mobile terminal methyls are represented by a central pair of peaks. At 40 °C, 16:0-22:6PE-d_{31} displays a spectrum characteristic of the H_{II} phase with edges at ±6 kHz (Figure 1c) that is reduced in width by the anticipated factor of $^1/_2$ in comparison to the L_α spectrum at 7.5 °C (*23*). We also assessed the phase behavior of the oleic acid-containing 16:0-18:1PE-d_{31} for which spectra are presented in Figure 1d,e. In contrast to 16:0-22:6PE-d_{31}, 16:0-18:1PE-d_{31} only showed formation of L_β and L_α phases over the temperature range of −10 to 40 °C studied. The spectra at −10 °C (Figure 1d) and 40 °C (Figure 1e), respectively, exemplify the behavior.

We compared the effect of equimolar CHOL on the phase behavior of hydrated 16:0-22:6PE-d_{31} vs 16:0-18:1PE-d_{31} (Figure 2). For 16:0-22:6PE-d_{31}/CHOL (Figure 2a) and 16:0-18:1PE-d_{31}/CHOL (Figure 2d) below 0 °C, the lamellar gel phase is maintained in the presence of equimolar CHOL. However, in the latter case the onset of fast axial rotation undergone by acyl chains in the liquid crystalline state is indicated at −10 °C by spectral shoulders at ±25 kHz. At 7.5 °C, a lamellar liquid crystalline spectrum with edges at ±23 kHz is observed for 16:0-22:6PE-d_{31}/CHOL (1:1 mol) bilayers (Figure 2b). The increase in broadening in comparison to 16:0-22:6PE-d_{31} (Figure 1b) shows that CHOL is increasing the order of the perdeuterated palmitoyl acyl chain consistent with the sterol's role in ordering phospholipids in the fluid phase. The sharpness of peaks within the spectrum may well signify that the membrane is l_o (*28*). Addition of equimolar CHOL to 16:0-22:6PE-d_{31} in the H_{II} phase at 40 °C (Figure 2c) results in a broadening of the spectrum to ±8 kHz compared to ±6 kHz for 16:0-22:6PE-d_{31} (Figure 1c). The broadening reveals that CHOL also exerts its ordering effect in the H_{II} phase. In contrast, 16:0-18:1PE-d_{31}/CHOL (1:1 mol) is lamellar at 40 °C. The spectrum (Figure 2e) is broadened to ±24 kHz relative to 16:0-18:1PE-d_{31} alone, as expected, which again demonstrates membrane ordering due to CHOL. The high definition of spectral peaks, moreover, agrees with the assessment that the l_o phase is formed by 16:0-18:1PE-d_{31}/CHOL when the concentration of cholesterol exceeds 35 mol % (*18*).

The spectra shown in Figures 1 and 2 are representative of data acquired over a wide temperature range for the different lipid combinations. To describe the trends observed in all of the acquired ^{2}H NMR spectra, the first moment M_1 was calculated using eq 2 and is plotted in Figure 3 as a function of temperature for 16:0-22:6PE-d_{31}, 16:0-22:6PE-d_{31}/CHOL (1:1 mol), 16:0-18:1PE-d_{31}, and 16:0-18:1PE-d_{31}/CHOL (1:1 mol). For 16:0-22:6PE-d_{31}, the L_β phase exists at temperatures <5 °C corresponding to $M_1 > 9.6 \times 10^4$

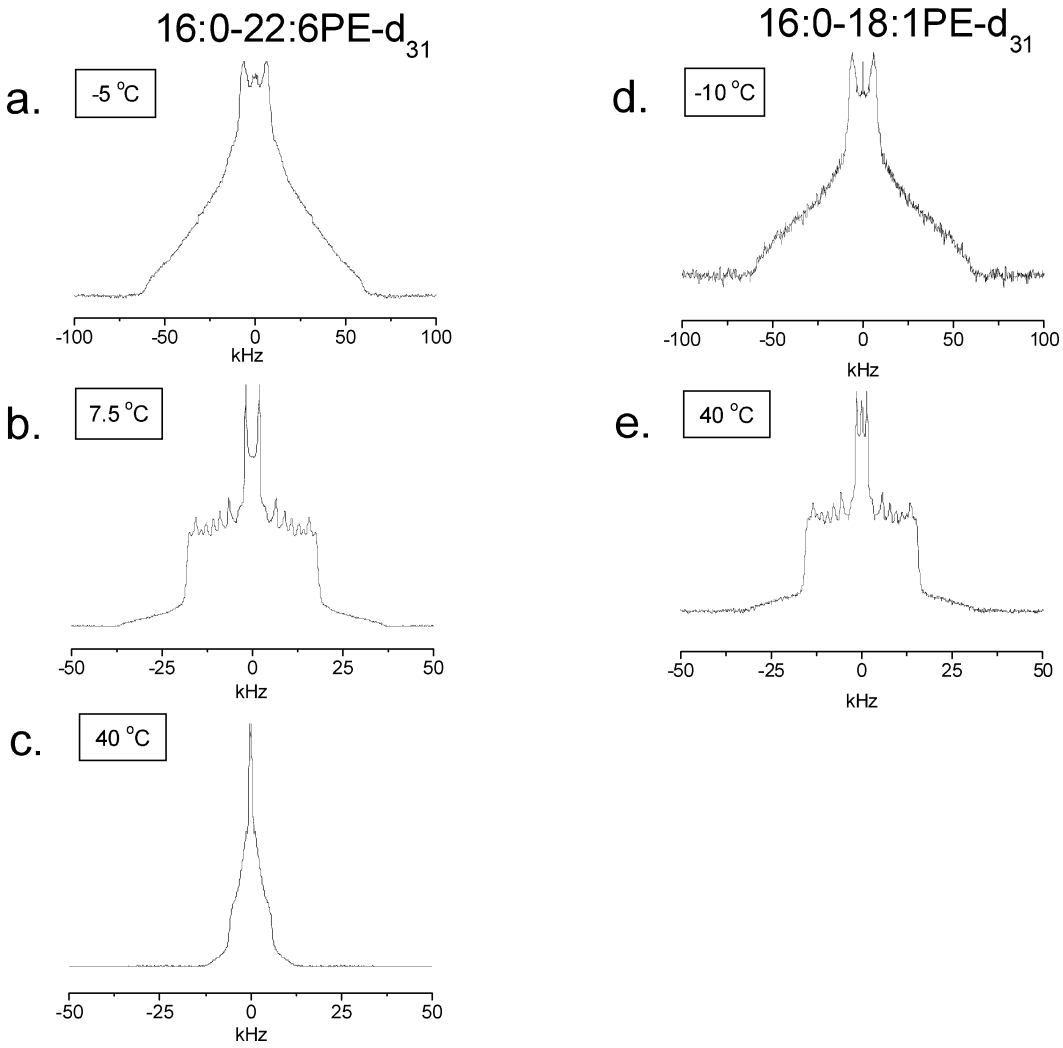

FIGURE 1: ^{2}H NMR spectra for 50 wt % aqueous dispersions in 50 mM Tris buffer (pH 7.5) of 16:0-22:6PE-d_{31} and 16:0-18:1PE-d_{31}. Spectra for 16:0-22:6PE-d_{31} were recorded at (a) −5, (b) 7.5, and (c) 40 °C. Spectra for 16:0-18:1PE-d_{31} were recorded at (d) −10 and (e) 40 °C.

s^{-1}. A narrow range of moments (6.3×10^4 $s^{-1} > M_1 > 5.9 \times 10^4$ s^{-1}), equivalent to a temperature range of 6−10 °C, characterizes the L_α phase. The abrupt drop in M_1 that accompanies the L_β−L_α change in state is ∼1 °C in width and takes place at 5 °C, which is comparable with our previously reported T_m = 2.2 °C for 16:0-22:6PE bilayers from DSC (*7*). Exact agreement between T_m values measured by the two methods is unlikely due to isotopic labeling and the different manner in which temperature is scanned. At higher temperature, a transition to the H_{II} phase ($M_1 \leq 3.3 \times 10^4$ s^{-1}) occurs spanning 10−15 °C. This phase remains up to 40 °C, which was the highest temperature recorded. Our earlier study of 1-stearoyl-2-docosahexaenoyl-*sn*-glycero-3-phosphoethanolamine (18:0-22:6PE) similarly found that the H_{II} phase was formed from 20 to 50 °C as detected by ^{31}P NMR spectroscopy (*29*).

The temperature dependence of the moments measured following the addition of equimolar CHOL to 16:0-22:6PE-d_{31} reveals the relatively modest change in phase behavior produced in the polyunsaturated PE. A chain melting transition temperature is still apparent. It is broadened to ∼5 °C in width and shifted down to a midpoint of −3 °C. The transition to H_{II} phase is less affected and remains centered at ∼13 °C. As expected, the M_1 values for 16:0-22:6PE-d_{31}/CHOL (1:1 mol) are generally higher in comparison to 16:0-22:6PE-d_{31}, reflecting the sterol-associated increase in order. The opposite effect is seen at low temperature (<−5 °C) where cholesterol disrupts molecular packing in the gel state bilayer. To the best of our knowledge, this is the first report of transition temperatures for 16:0-22:6PE-d_{31} and 16:0-22:6PE-d_{31}/CHOL (1:1 mol) detected with ^{2}H NMR spectroscopy.

For 16:0-18:1PE-d_{31}, only the L_β−L_α phase transition occurs within the temperature range examined. The moments $M_1 > 10.7 \times 10^4$ s^{-1} measured at temperatures ≤22.5 °C signify the L_β state, while $M_1 < 6.42 \times 10^4$ s^{-1} found 25−40 °C corresponds to the L_α phase. The sharp change in M_1 between L_β and L_α states centered at 23.4 °C is close to our previous finding of T_m = 25.5 °C from DSC (*7*). Formation of the H_{II} phase by 16:0-18:1PE has been observed outside the currently investigated temperature range at ∼70 °C by ^{2}H NMR, IR, DSC, and XRD (*18*, *30*). Inspection of M_1 as a function of temperature for 16:0-18:1PE-d_{31}/CHOL (1:1 mol) reveals that M_1 values gradually decrease [(10−7) × 10^4 s^{-1}]. There is no longer a sharp discontinuity. This implied broadening to near obliteration of the main chain melting phase transition is typical of the effect that incorporation of 50 mol % cholesterol has on phospholipid

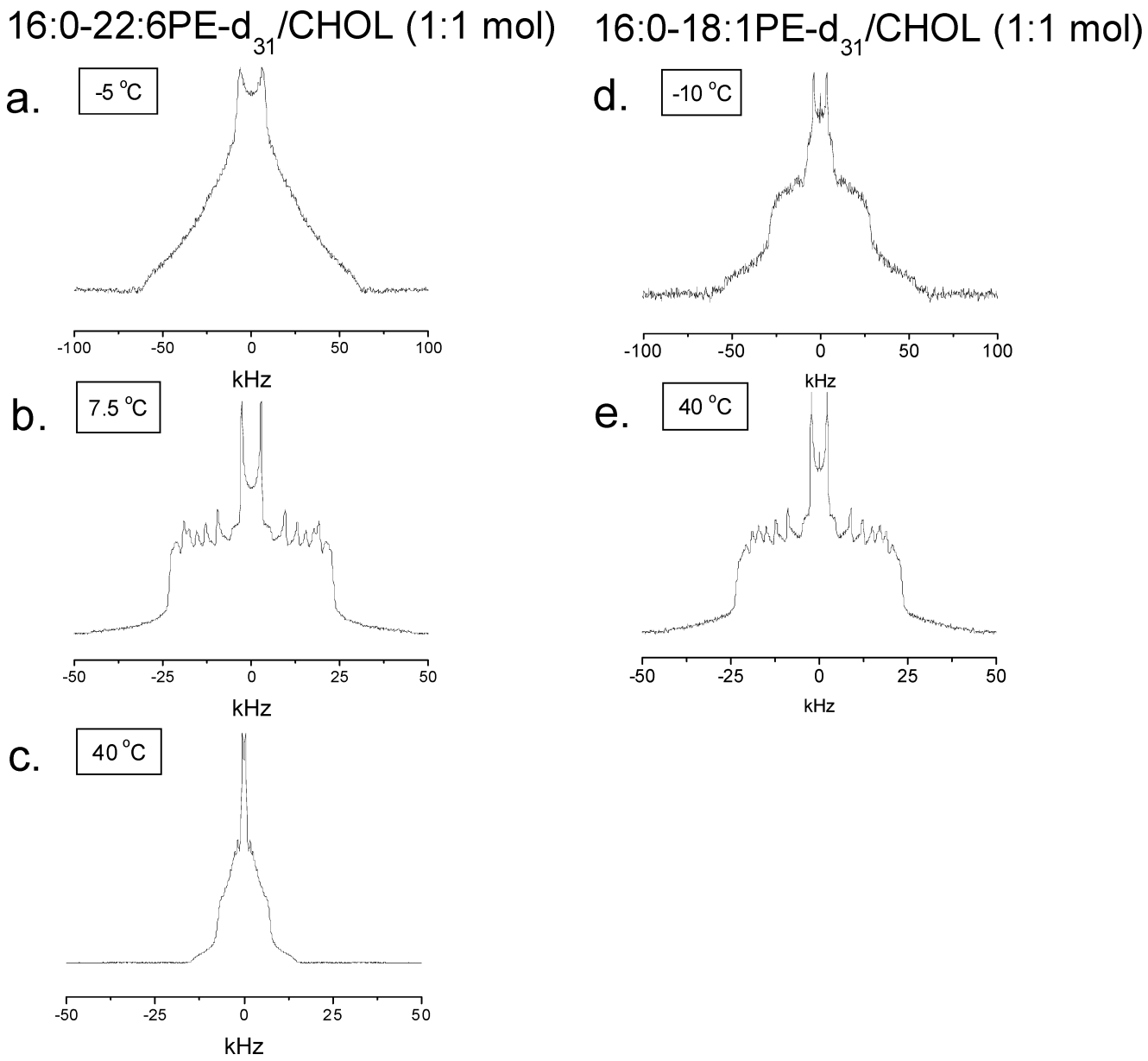

FIGURE 2: ^{2}H NMR spectra for 50 wt % aqueous dispersions in 50 mM Tris buffer (pH 7.5) of 16:0-22:6PE-d_{31}/CHOL (1:1 mol) and 16:0-18:1PE-d_{31}/CHOL (1:1 mol). Spectra for 16:0-18:1PE-d_{31}/CHOL (1:1 mol) were recorded at (a) −5, (b) 7.5, and (c) 40 °C. Spectra for 16:0-18:1PE-d_{31}/CHOL (1:1 mol) were recorded at (d) −10 and (e) 40 °C.

bilayers (*3*). The retention of the well-defined phase transition seen here in 16:0-22:6PE-d_{31} despite the addition of 50 mol % sterol identifies a major distinction in interaction of cholesterol with the polyunsaturated PE.

Cholesterol's Ordering Effect on 16:0-22:6PE-d_{31} vs 16:0-18:1PE-d_{31}. Ideally we would compare the effect of CHOL on 16:0-22:6PE-d_{31} vs 16:0-18:1PE-d_{31} bilayers at identical temperature. The moments plotted against temperature in Figure 3 reveal, however, that the polyunsaturated and monounsaturated phospholipids do not adopt the L_α phase at the same temperature. Our compromise is to compare under conditions of equivalent phase at two different temperatures. Table 1 presents M_1 and the average order parameter $\bar{S}_{CD}$ calculated via eq 2 for 16:0-22:6PE-d_{31} and 16:0-22:6PE-d_{31}/CHOL (1:1 mol) at 7.5 °C and for 16:0-18:1PE-d_{31} and 16:0-18:1PE-d_{31}/CHOL (1:1 mol) at 40 °C. Both systems are then lamellar and liquid crystalline. The indication that order in 16:0-22:6PE-d_{31} is higher than in 16:0-18:1PE-d_{31}, it should be noted, we attribute to the difference in temperature. The increase in $\bar{S}_{CD}$ upon the addition of equimolar CHOL to 16:0-22:6PE-d_{31} (7.5 °C) represents a change in $\bar{S}_{CD}$ of 22%. In contrast, $\bar{S}_{CD}$ is increased by 33% in 16:0-18:1PE-d_{31}/CHOL (1:1 mol) relative to 16:0-18:1PE-d_{31} (40 °C).

The ^{2}H NMR spectra for 16:0-22:6PE-d_{31} and 16:0-18:1PE-d_{31} at 7.5 and 40 °C, respectively, in the absence and presence of equimolar CHOL were FFT depaked to enhance spectral resolution (Figure 4) (*24*). The depaked spectra consist of an outermost composite doublet and five to six well-resolved doublets. The composite doublet is due to ordered methylenes in the upper part of the acyl chain while the individual doublets represent, sequentially with reduced splitting, the disordered methylenes and terminal methyl in the lower portion of the acyl chain. Exploiting this improvement in resolution, the depaked data were used to create smoothed order parameter profiles by assigning equal

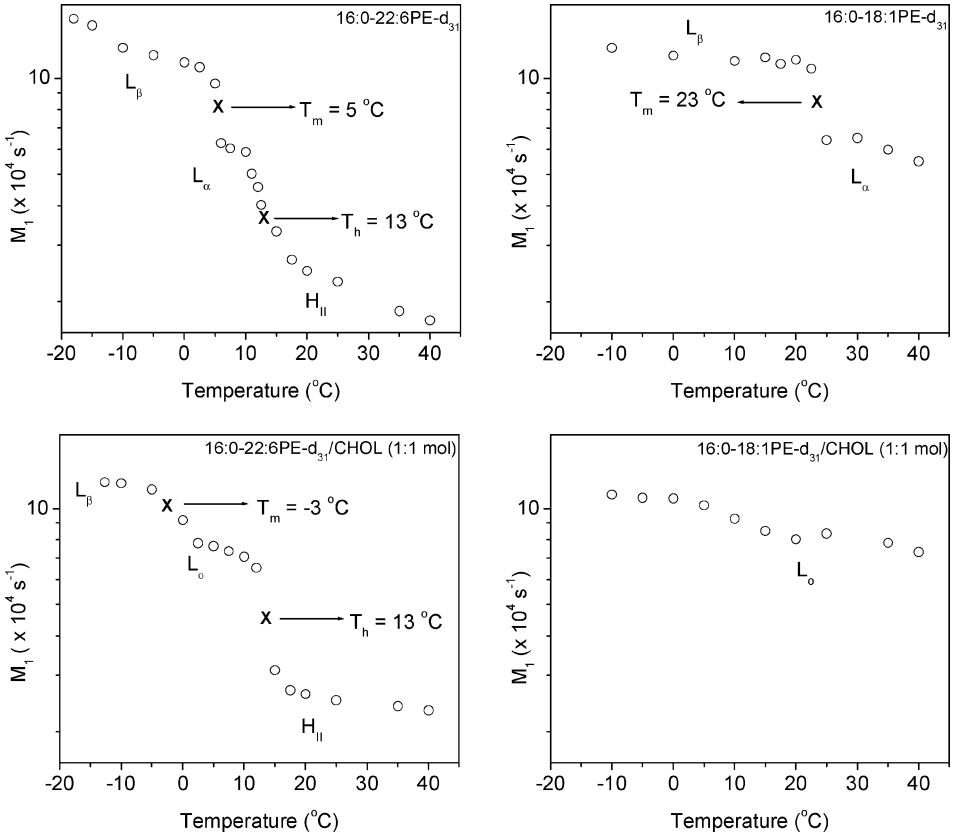

FIGURE 3: Variation in the first moment M_1 (eq 1) as a function of temperature for 50 wt % aqueous dispersions in 50 mM Tris buffer (pH 7.5) of 16:0-22:6PE-d_{31}, 16:0-22:6PE-d_{31}/CHOL (1:1 mol), 16:0-18:1PE-d_{31}, and 16:0-18:1PE-d_{31}/CHOL (1:1 mol). M_1 is plotted logarithmically for clarity, and the values are subject to ±2% uncertainty. The transition temperatures T_m and T_h, designated by x, are the midpoint of the sharp drops in moment that accompany the respective gel-to-liquid crystalline and lamellar-to-inverted hexagonal phase transitions.

Table 1: Data Derived from ^{2}H NMR Spectra for Liquid Crystalline Bilayers of 16:0-22:6PE-d_{31} and 16:0-22:6PE-d_{31}/CHOL (1:1 mol) at 7.5 °C and 16:0-18:1PE-d_{31} and 16:0-18:1PE-d_{31}/CHOL (1:1 mol) at 40 °C

lipid composition	M_1 ($\times 10^4$ s^{-1})	$\bar{S}_{CD}$
16:0-22:6PE-d_{31}	6.04	0.198
16:0-22:6PE-d_{31}/CHOL (1:1 mol)	7.36	0.241
16:0-18:1PE-d_{31}	5.51	0.181
16:0-18:1PE-d_{31}/CHOL (1:1 mol)	7.31	0.240

integrated intensity to each methylene group in the perdeuterated *sn*-1 palmitoyl chain and assuming a monotonic decrease in order toward the terminal methyl (*25*).

The order parameters calculated as a function of acyl chain position for 16:0-22:6PE-d_{31} and 16:0-22:6PE-d_{31}/CHOL (1:1 mol) at 7.5 °C (Figure 5A) and for 16:0-18:1PE-d_{31} and 16:0-18:1PE-d_{31}/CHOL (1:1 mol) at 40 °C (Figure 5B) are shown in Figure 5. All four profiles show a similar qualitative trend marked by a characteristic plateau of approximately constant order in the upper part of the perdeuterated acyl chain (C2−9) with a subsequent progressive decrease in order toward the middle of the bilayer (C10−16). The addition of sterol to both phospholipids results in an increase in S_{CD} for each carbon position. The effect is more pronounced in the plateau region of almost uniform order in the upper part of the acyl chain toward the surface of the bilayer for both 16:0-22:6PE-d_{31} and 16:0-18:1PE-d_{31}. However, quantitative differences do exist between profiles. The elevation in order of the plateau region upon the addition of CHOL is greater for 16:0-18:1PE-d_{31} than for 16:0-22:6PE-d_{31}. For example, S_{CD} changes from ∼0.30 to ∼0.37 at carbon position 2 in 16:0-22:6PE-d_{31} whereas 16:0-18:1PE-d_{31} displays a change in order from S_{CD} ∼0.25 to ∼0.38 at the same position. These changes in S_{CD} constitute an increase in order of 23% for 16:0-22:6PE-d_{31} and 52% for 16:0-18:1PE-d_{31} upon the addition of equimolar CHOL. Clearly the effect of CHOL on 16:0-22:6PE-d_{31} is less than on 16:0-18:1PE-d_{31} bilayers, consistent with the behavior observed in $\bar{S}_{CD}$ (Table 1).

Solubility of Cholesterol in 16:0-22:6PE vs 16:0-18:1PE. The average order parameters (Table 1) and profiles of order (Figure 5) establish that the restriction to chain mobility associated with addition of 50 mol % cholesterol is substantially lower in 16:0-22:6PE-d_{31} bilayers relative to 16:0-18:1PE-d_{31}. More profoundly, a transition between bilayer gel and liquid crystalline states was still apparent in the graph of M_1 vs temperature obtained from ^{2}H NMR spectroscopy of 16:0-22:6PE-d_{31} in the presence of sterol (Figure 3). This is in distinct contrast to 16:0-18:1PE where, as is normally the case, equimolar cholesterol nearly abolishes the transition. A marked reduction in solubility of CHOL for 16:0-22:6PE-d_{31} is a possible interpretation. To investigate this possibility, low- and wide-angle XRD patterns were acquired at 7.5 °C for 16:0-22:6PE and compared to 16:0-18:1PE at 40 °C. The basis of the approach is to look for diffraction peaks due to solid cholesterol excluded from the bilayer when the solubility limit has been exceeded (*4*, *20*).

Integrated radial intensity profiles as a function of reciprocal space ($q = 4\pi \sin\theta/\lambda$) for 16:0-22:6PE/CHOL samples

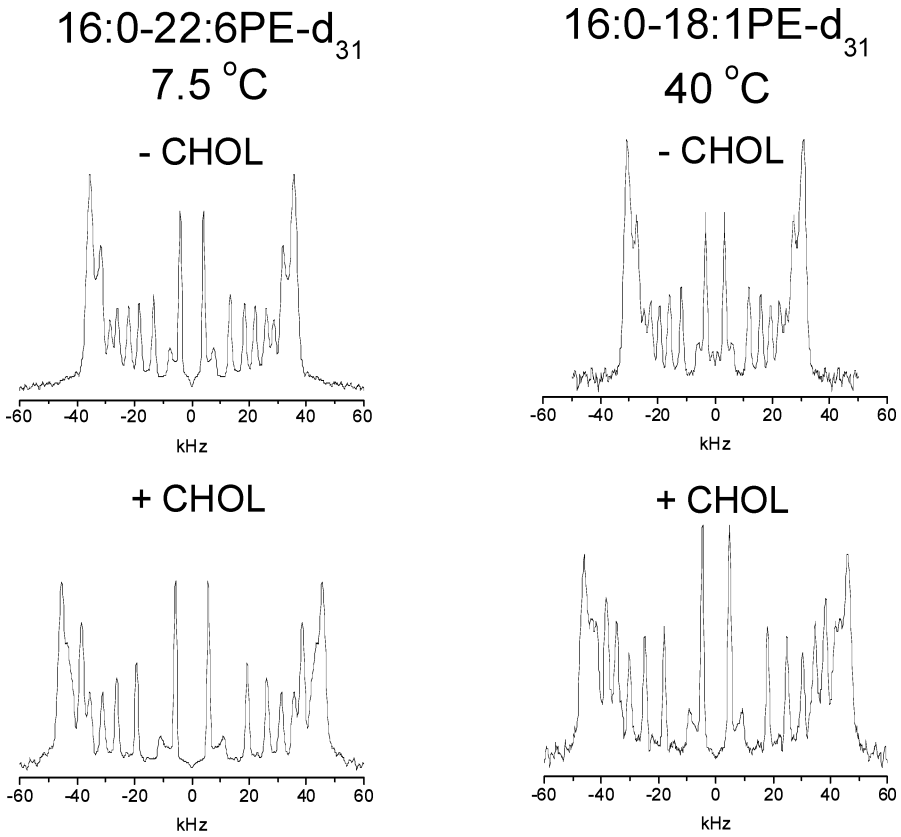

FIGURE 4: Depaked spectra for 16:0-22:6PE-d_{31} and 16:0-18:1PE-d_{31} bilayers in the absence or presence of equimolar CHOL. 16:0-22:6PE-d_{31} and 16:0-22:6PE-d_{31}/CHOL (1:1 mol) spectra were recorded at 7.5 °C. 16:0-18:1PE-d_{31} and 16:0-18:1PE-d_{31}/CHOL (1:1 mol) spectra were recorded at 40 °C.

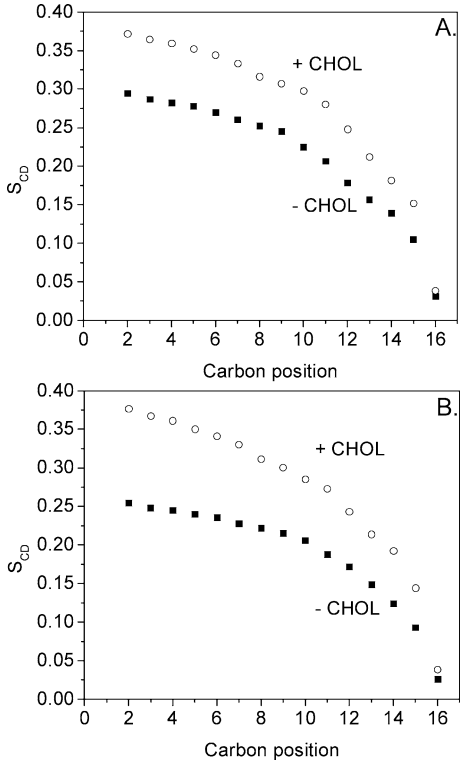

FIGURE 5: Smoothed order parameter profiles generated from depaked spectra for bilayers of (A) 16:0-22:6PE-d_{31} (■) and 16:0-22:6PE-d_{31}/CHOL (1:1 mol) (○) at 7.5 °C and (B) 16:0-18:1PE-d_{31} (■) and 16:0-18:1PE-d_{31}/CHOL (1:1 mol) (○) at 40 °C.

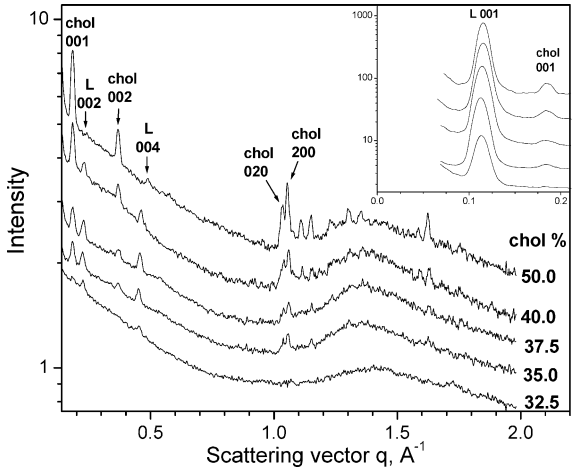

FIGURE 6: Phase behavior of 16:0-22:6PE in combination with cholesterol at 7.5 °C as revealed by low- and wide-angle X-ray diffraction. Samples were prepared at 50% (w/w) total lipid in 50 mM Tris (pH 7.5). The cholesterol concentration in each sample is indicated as mole percent. The inset shows the first-order low-angle reflections from the bulk lamellar phase (L 001, d = 55 Å) and from the phase-separated lamellar crystal of cholesterol monohydrate (chol 001, d = 34 Å). $I-q$ plots are offset along the ordinate for clarity.

containing various amounts of added sterol are presented in Figure 6. The plot is cropped from q = 0.15−2.0 Å^{-1} to focus on the region where second-order peaks that can be assigned unambiguously arise from cholesterol monohydrate or anhydrous cholesterol (*26*). Low-angle reflections from the bulk phase [L 002 and L 004 (and L 001 in the inset)] confirm that this is of the lamellar type at 7.5 °C. The $I-q$ plots reveal that the 002, 020, and 200 peaks at 0.37 Å^{-1} (d = 17 Å), 1.03 Å^{-1} (d = 6.08 Å), and 1.04 Å^{-1} (d = 6.02 Å)

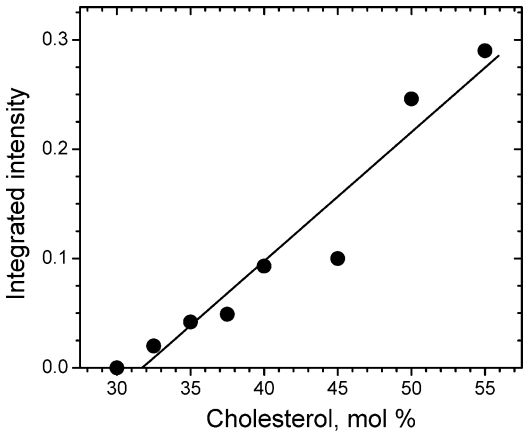

FIGURE 7: Cholesterol-carrying capacity of the lamellar liquid crystalline phase of 16:0-22:6PE at 7.5 °C. Summed diffraction intensity associated with the second-order reflections (chol 002, chol 020, and chol 200 in Figure 6) from cholesterol monohydrate and normalized with respect to fluid acyl chain scatter (see Experimental Procedures) is shown as a function of mole percent cholesterol in 16:0-22:6 PE dispersed in 50 mM Tris (pH 7.5).

respectively, from crystalline cholesterol in the monohydrate form are barely observable at 32.5 mol % cholesterol and that they grow in intensity as cholesterol concentration increases. To quantify the concentration at which sterol exclusion from 16:0-22:6PE begins, the summed integrated intensities of these three second-order reflections (normalized with respect to the lipid wide-angle peak centered at $q \sim 1.4$ Å^{-1}) are plotted as a function of mole percent cholesterol in Figure 7. Linear extrapolation to zero integrated intensity intercepts the abscissa at 32 ± 3 mol % CHOL. We identify this concentration as the solubility of cholesterol in the lamellar liquid crystalline phase of 16:0-22:6PE. Our result for this saturated−polyunsaturated PE is greatly reduced compared to the value of 51 mol % that we measured (data not shown) and that was previously reported for saturated−monounsaturated 16:0-18:1PE (*20*).

DISCUSSION

Our previous findings led us to suggest that 16:0-18:1PE does not promote lipid raft formation in 16:0-18:1PE/SM/CHOL (1:1:1 mol) but that substitution of polyunsaturated DHA for monounsaturated oleic acid in PE may trigger local phase separation (*7*). To elucidate the molecular mechanism by which DHA promotes lateral segregation, we conducted experiments in the present study characterizing the molecular interactions prevailing in 16:0-22:6PE-d_{31} and 16:0-22:6PE-d_{31}/CHOL (1:1 mol) in comparison to 16:0-18:1PE-d_{31} and 16:0-18:1PE-d_{31}/CHOL (1:1 mol).

16:0-22:6PE Phase Behavior. Numerous studies have established that PEs can adopt nonlamellar phases (*18*, *30*, *31*). The driving force for the formation of H_{II} structures by PEs is the negative stress curvature that results from a relatively small headgroup size as well as the ability to hydrogen bond with adjacent polar headgroups (*32*−*34*). The lowering of the temperature of the L_α to H_{II} transition seen in our ^{2}H NMR moment data for 16:0-22:6PE-d_{31} ($T_h \approx 13$ °C) relative to less unsaturated PEs (*23*, *30*, *31*) complies with the well accepted increase in propensity to form the H_{II} phase when multiple doubles are present (*35*). The ability to form the H_{II} phase with 16:0-22:6PE-d_{31} may be physiologically important (*34*). For instance, it has been reported that nonbilayer phases may attenuate or potentiate protein kinase C activity (*36*) and may influence the organization of tight junctions (*37*). Model membrane studies also show that the L_α-to-H_{II} transition of PEs may be relevant to membrane fusion events (*38*). Additionally, there is evidence proposing the existence of nonbilayer phases in biological membranes, which have implications for human antiphospholipid syndrome (*39*).

Numerous DSC and NMR studies, most of which have used saturated PCs, have clearly demonstrated that incorporation of the sterol at high concentrations into various phospholipids abolishes the gel-to-liquid crystalline phase transition (*28*, *40*, *41*). However, inspection of the M_1 vs temperature (Figure 3) plot for 16:0-22:6PE-d_{31}/CHOL (1:1 mol) reveals that the T_m for 16:0-22:6PE-d_{31} is retained despite the presence of equimolar cholesterol. This finding suggested that cholesterol did not disrupt the packing properties of the DHA-containing PE in the gel state to the same extent as 16:0-18:1PE-d_{31} where equimolar cholesterol essentially eliminates T_m (Figure 3). We hypothesize that a lowered solubility of sterol in the polyunsaturated case was responsible. A precedent for such a suggestion is set by earlier investigations of dipolyunsaturated PCs. DSC detected minimal effect of equimolar cholesterol on the gel-to-liquid crystalline transition temperature of 22:6-22:6PC membranes (*42*), which our subsequent XRD results established may be explained by a solubility of ≤17 mol % for the sterol therein (*4*).

Ordering Effect of Cholesterol. Our ^{2}H NMR results reveal the perturbation to acyl chain organization produced when equimolar cholesterol was added to 16:0-22:6PE-d_{31}. The spectral moments plotted in Figure 3 reflect the anticipated increase in membrane order in the liquid crystalline state. The effect is maintained in the H_{II} as well as the lamellar phase. Comparison with the moments for 16:0-18:1PE-d_{31} and 16:0-18:1PE-d_{31}/CHOL (1:1 mol), however, demonstrates that the impact of the sterol is reduced for the DHA-containing phospholipid. The change in average order parameters $\bar{S}_{CD}$ measured for 16:0-22:6PE-d_{31} at 7.5 °C vs 16:0-18:1PE-d_{31} at 40 °C due to the addition of equimolar cholesterol can be seen in Table 1. These two different temperatures were chosen so that both systems were lamellar. The temperature dependence of moments shows that such a situation is not satisfied at a single temperature (Figure 3). The increase in order was 22% for 16:0-22:6PE-d_{31}, whereas for 16:0-18:1PE-d_{31} order increased by 33%, which is comparable to a previous report of 35% found for 16:0-18:1PE-d_{31}/45 mol % CHOL at 35 °C (*18*). A smaller sterol-associated effect for 16:0-22:6PE-d_{31} bilayers than for 16:0-18:1PE-d_{31} bilayers is accordingly apparent in the profiles of order presented in Figure 5. Cholesterol similarly appears to exert a somewhat reduced influence on acyl chain organization in 16:0-22:6PE-d_{31} in the H_{II} phase. The average order parameters determined from spectra for 16:0-22:6PE-d_{31} and 16:0-22:6PE-d_{31}/CHOL (1:1 mol) at 40 °C are $\bar{S}_{CD} = 0.115$ and 0.152, respectively, representing an increase of 32% in $\bar{S}_{CD}$. An increase of 45% in order was previously reported for 16:0-18:1PE in the H_{II} phase upon the incorporation of 45 mol % cholesterol at 70 °C (*18*).

Cholesterol Solubility. The diminution in effect on membrane phase behavior and ordering that our ^{2}H NMR data

indicated accompanies the addition of equimolar cholesterol to 16:0-22:6PE-d_{31} vs 16:0-18:1PE-d_{31} led us to ascertain whether less sterol incorporated into the DHA-containing phospholipid. Although our experiments showed formation of the H_{II} phase by 16:0-22:6PE-d_{31} in the physiological temperature range, which may have biological implications as discussed before, we decided to investigate cholesterol's solubility in the lamellar phase at 7.5 °C. In the presence of other biologically relevant lipids, such as sphingomyelin (*7*), 16:0-22:6PE-d_{31} adopts the lamellar liquid crystalline phase, and thus, determination of cholesterol solubility in this state mimics the in vivo condition more accurately.

A solubility of 32 ± 3 mol % for cholesterol in 16:0-22:6PE bilayers at 7.5 °C was identified on the basis of the XRD data presented in Figures 6 and 7. This result is, we believe, the first report of sterol solubility in a heteroacid *sn*-1 saturated, *sn*-2 polyunsaturated PE. In contrast, bilayers composed of 16:0-18:1PE at 40 °C were found to have a solubility to cholesterol of ~51 mol %, which agrees with the result obtained in an earlier work (*20*). The implication is that the introduction of polyunsaturation into the *sn*-2 chain of PE lowers the ability of cholesterol to incorporate into the membrane. Such a finding is consistent with the smaller response to cholesterol detected in 16:0-22:6PE-d_{31} by ^{2}H NMR relative to 16:0-18:1PE-d_{31}. Earlier studies have demonstrated that sterol solubility in phospholipids is influenced by both degree of acyl chain unsaturation and headgroup structure (*43*). It was recently demonstrated that, in particular, the solubility of cholesterol in PC bilayers is sensitive to the presence of polyunsaturation (*4*, *10*, *44*). In dipolyunsaturated 1,2-diarachidonoyl-*sn*-glycero-3-phosphocholine (20:4-20:4PC) and 1,2-didocosahexaenoyl-*sn*-glycero-3-phosphocholine (22:6-22:6PC) <15 mol % cholesterol could be accommodated within the membrane, although in *sn*-1 saturated, *sn*-2 polyunsaturated 1-stearoyl-2-arachidonoyl-*sn*-glycero-3-phosphocholine (18:0-20:4PC) and 1-stearoyl-2-docosahexaenoyl-*sn*-glycero-3-phosphocholine (18:0-22:6PC) the solubility remains >50 mol % irrespective of the degree of unsaturation in the *sn*-2 chain. Factors associated with the headgroup that affect the limit on membrane incorporation of sterol are the presence of charge on the headgroup and interheadgroup hydrogen bonds (*43*). The average solubility reported for cholesterol in disaturated 14:0 bilayers is in the following order: PC > PG ~ PE > PS (*43*).

The lateral organization of cholesterol within a membrane and its solubility therein has been described by the umbrella model developed with Monte Carlo simulations (*45*). The gist of the model is that cholesterol multibody interactions are energetically unfavorable. Phospholipid−cholesterol mixtures at critical ratios form highly regular distributions in order to minimize sterol−sterol interactions. Polar phospholipid headgroups act as "umbrellas" by preventing the unfavorable free energy of contact of the sterol with interfacial water. An increase in sterol above the critical ratios results in a large increase in cholesterol potential energy that favors its precipitation from the bilayer. By this model the observation of a lower limit to cholesterol solubility for 16:0-18:1PE (51 mol %) vs 1-palmitoyl-2-oleoyl-*sn*-glycero-3-phosphocholine (16:0-18:1PC) (66 mol %) was attributed to the smaller PE headgroup, which shields the interior of the bilayer from water less effectively than PC. We have further argued that highly disordered polyunsaturated acyl chains may analogously render the bilayer less soluble to cholesterol because of the reduction in shielding by headgroups that will accompany the increase in area/molecule produced (*4*, *10*). In the case of 16:0-22:6PE, reduced cholesterol solubility may then be reconciled on the basis of decreased headgroup shielding. Whereas polyunsaturated fatty acids (PUFAs) are required at both *sn*-1 and *sn*-2 positions in PC (*4*) to markedly limit bilayer incorporation of the sterol, our results for 16:0-22:6PE demonstrate that a polyunsaturated *sn*-2 chain is sufficient in PE. Reservations about interpretation in terms of the umbrella model, however, should be borne in mind. An example is the lower hydration of the interfacial region indicated for PE than PC (*46*), which would argue against a reduction in sterol solubility because accessibility to water is increased in PE bilayers.

Cholesterol−DHA Interactions. There is a small body of experimental data examining cholesterol−DHA interactions that suggests the sterol has diminished affinity for the polyunsaturated acyl chain compared to a monounsaturated or saturated acyl chain at the *sn*-2 position in heteroacid phospholipids with a saturated *sn*-1 chain. For instance, pressure−area isotherms of monolayers composed of 18:0-18:1PC or 18:0-22:6PC in the presence of cholesterol indicate that the sterol interacts unfavorably with the DHA acyl chain (*47*). The unfavorable interaction is attributed to steric incompatibility between the rigid steroid moiety and the highly disorganized DHA acyl chain, which may have biological implications for the lipid microdomain as well as raft formation. In membranes containing 16:0-22:6PE and cholesterol, the polyunsaturated fatty acyl chain at the *sn*-2 position may promote lateral phase segregation into PUFA-rich/sterol-poor and PUFA-poor/sterol-rich regions. Preliminary results presented in our earlier investigation of 16:0-22:6PE/SM/CHOL support this proposal (*7*). Pressure−area isotherms, DSC, and ^{2}H NMR spectroscopy indicate phase separation that was not seen when monounsaturated 16:0-18:1PE was substituted for the polyunsaturated phospholipid. Further experiments on 16:0-22:6PE/SM/CHOL mixed membranes are currently underway and will be the subject of a forthcoming report.

Conclusion. In summary, ^{2}H NMR measurements establish that the addition of equimolar cholesterol has less of an effect on the phase behavior and on the order of the *sn*-1 acyl chain in the liquid crystalline state of 16:0-22:6PE-d_{31} vs 16:0-18:1PE-d_{31}. Corroborating XRD experiments demonstrate that cholesterol has a reduced solubility in 16:0-22:6PE than in 16:0-018:1PE bilayers, providing a rationale for the smaller impact of the sterol on the DHA-containing phospholipid. We propose that a reduced affinity of cholesterol for 16:0-22:6PE may trigger lateral segregation into DHA-poor/sterol-rich and DHA-rich/sterol-poor microdomains which would have implications for lipid raft formation and protein function.

ACKNOWLEDGMENT

We thank Dr. Michel Lafleur for providing ^{2}H NMR data on 16:0-18:1PE-d_{31} for comparison.

REFERENCES

1. Lange, Y., Swaisgood, M. H., Ramos, B. V., and Stack, T. L. (1989) *J. Biol. Chem. 264*, 3786−3793.

2. Straume, M. (1987) *Biochemistry 26*, 5121−5126.
3. Finegold, L., Ed. (1993) *Cholesterol in Model Membranes*, CRC Press, Boca Raton, FL.
4. Brzustowicz, M. R., Cherezov, V., Zerouga, M., Caffrey, M., Stillwell, W., and Wassall, S. R. (2002) *Biochemistry 41*, 12509−12519.
5. Huster, D., Arnold, K., and Gawrisch, K. (1998) *Biochemistry 37*, 17299−17308.
6. Shaikh, S. R., Dumaual, A. C., Jenski, L. J., and Stillwell, W. (2001) *Biochim. Biophys. Acta 1512*, 317−322.
7. Shaikh, S. R., Brzustowicz, M. R., Gustafson, N., Stillwell, W., and Wassall, S. R. (2002) *Biochemistry 41*, 10593−10602.
8. Stillwell, W. (2000) *Curr. Org. Chem. 4*, 1169−1183.
9. Mitchell, D. C., and Litman, B. J. (1998) *Biophys. J. 74*, 879−891.
10. Brzustowicz, M. R., Cherezov, V., Caffrey, M., Stillwell, W., and Wassall, S. R. (2002) *Biophys. J. 82*, 285−298.
11. Simons, K., and Ikonen, E. (1997) *Nature 387*, 569−572.
12. Brown, D. A., and Rose, J. K. (1992) *Cell 67*, 533−544.
13. Brown, D. A., and London, E. (2000) *J. Biol. Chem. 275*, 17221−17224.
14. Ipsen, J. H., Karlstrom, G., Mouritsen, O. G., Wennerstrom, H., and Zuckerman, M. J. (1987) *Biochim. Biophys. Acta 905*, 162−172.
15. Melkonian, K. A., Ostermeyer, A. G., Chen, J. Z., Roth, M. G., and Brown, D. A. (1999) *J. Biol. Chem. 274*, 3910−3917.
16. Van Dijck, P. M. W., De Kruijff, B. B. K., Van Deenen, L. L. M., De Gier, J., and Demel, R. A. (1976) *Biochim. Biophys. Acta 455*, 576−587.
17. Niu, S.-L., and Litman, B. J. (2002) *Biophys. J. 83*, 3408−3415.
18. Pare, C., and Lafleur, M. (1998) *Biophys. J. 74*, 899−909.
19. Zerouga, M., Stillwell, W., Stone, J., Powner, A., and Jenski, L. (1996) *Anticancer Res. 16*, 2863−2868.
20. Huang, J., Buboltz, J. T., and Feigenson, G. W. (1999) *Biochim. Biophys. Acta 1417*, 89−100.
21. McCabe, M. A., Griffith, G. L., Ehringer, W. D., Stillwell, W., and Wassall, S. R. (1994) *Biochemistry 33*, 7203−7210.
22. Davis, J. H. (1983) *Biochim. Biophys. Acta 737*, 117−171.
23. Thurmond, R. L., Lindblom, G., and Brown, M. R. (1993) *Biochemistry 32*, 5394−5410.
24. McCabe, M. A., and Wassall, S. R. (1997) *Solid-State Nucl. Magn. Reson. 10*, 53−61.
25. Lafleur, M., Fine, B., Sternin, E., Cullis, P. R., and Bloom, M. (1989) *Eur. Biophys. J. 56*, 1037−1041.
26. Craven, B. M. (1976) *Nature 260*, 727−729.
27. Wassall, S. R., Thewalt, J. L., Wong, L., Gorrissen, H., and Cushley, R. J. (1986) *Biochemistry 25*, 319−326.
28. Vist, M. R., and Davis, J. H. (1990) *Biochemistry 29*, 451−464.
29. Shaikh, S. R., Brzustowicz, M. R., Stillwell, W., and Wassall, S. R. (2001) *Biochem. Biophys. Res. Commun. 286*, 758−763.
30. Epand, R. M., and Bottega, R. (1987) *Biochemistry 26*, 1820−1825.
31. Harlos, K., and Eibl, H. (1981) *Biochemistry 20*, 2888−2892.
32. Cullis, P. R., and De Kruijff, B. (1978) *Biochim. Biophys. Acta 507*, 207−218.
33. Gruner, S. M., Cullis, P. R., Hope, M. J., and Tilcock, C. P. (1985) *Annu. Rev. Biophys. Biophys. Chem. 14*, 211−238.
34. Gawrisch, K., and Holte, L. (1996) *Chem. Phys. Lipids 81*, 105−116.
35. Lafleur, M., Bloom, M., Eikenberry, E. F., Gruner, S. M., Han, Y., and Cullis, P. R. (1996) *Biophys. J. 70*, 2747−2757.
36. Slater, S. J., Kelly, M. B., Taddeo, F. J., Ho, C., Rubin, E., and Stubbs, C. D. (1994) *J. Biol. Chem. 269*, 4866−4871.
37. Wegener, J., and Galla, H. J. (1996) *Chem. Phys. Lipids 81*, 229−255.
38. Siegel, D. P., and Epand, R. M. (1997) *Biophys. J. 73*, 3089−3111.
39. Aguilar, L., Ortega-Pierres, G., Campos, B., Fonseca, R., Ibanez, M., Wong, C., Farfan, N., Naciff, J., Kaetzel, M., Dedman, J., and Baeza, I. (1999) *J. Biol. Chem. 264*, 25193−25196.
40. McMullen, T. P. W., and McElhaney, R. N. (1996) *Curr. Opin. Colloid Interface Sci. 1*, 83−90.
41. Thewalt, J. L., and Bloom, M. (1992) *Biophys. J. 63*, 1176−1181.
42. Kariel, N., Davidson, E., and Keough, K. M. W. (1991) *Biochim. Biophys. Acta 1062*, 70−76.
43. Bach, D., and Wachtel, E. (2003) *Biochim. Biophys. Acta 1610*, 187−197.
44. Brzustowicz, M. R., Stillwell, W., and Wassall, S. R. (1999) *FEBS Lett. 451*, 197−202.
45. Huang, J., and Feigenson, G. (1999) *Biophys. J. 76*, 2142−2157.
46. Lewis, R. N., and McElhaney, R. N. (1993) *Biophys. J. 64*, 1081−1096.
47. Zerouga, M., Jenski, L. J., and Stillwell, W. (1995) *Biochim. Biophys. Acta 1236*, 266−272.

BI034931+